Iranian Journal of Science & Technology, Transaction A, Vol. 32, No. A1
Printed in The Islamic Republic of Iran, 2008

INVESTIGATION ON THE FLUX-BASED TORQUE-RIPPLE BEHAVIOR IN DTC BASED INDUCTION MOTOR DRIVES[*]

SH. KABOLI[**], M. R. ZOLGHADRI, S. HAGHBIN AND P. ESKANDARI

Electrical Engineering Department, Sharif University of Technology, Tehran, I. R. of Iran
Email: kaboli@sharif.edu

Abstract – The efficiency of induction motors decreases at light loads. Efficiency optimizer control systems adjust the motor flux value to achieve the best efficiency in a wide range of load variations. Reduced flux operation has some other benefits such as power factor improvement and torque ripple reduction. The latter is an important issue in a direct torque controlled induction motor drive. In this paper, the effect of flux reference value on the torque ripple of a direct torque controlled induction motor is analyzed. The effect of flux value on torque ripple in a wide range of speed variations is investigated. Simulation and the experimental results presented justify the validity of the theoretical analysis about torque ripple.

Keywords – Induction motor drive, direct torque control, torque ripple, predictive controller

1. INTRODUCTION

Induction motors consume more than 60% of industrial electricity [1]. This is the origin of considerable efforts to improve their efficiency through using high quality materials and excellent design procedures in the manufacturing process and expert control algorithms in the operation process. Adaptation of the motor flux with load variations is the main approach for efficiency optimization during the operation of AC drives. The nominal value of flux optimizes the operation of the drive in its nominal operating point. But at light loads, using nominal flux results in a decrease in the power factor and the efficiency of the motor. Efficiency optimizer systems adjust the motor flux value to maximize the motor efficiency during load variations [2].

Since the first developments of the direct torque control (DTC) concept [3], [4], it has been used in many AC drive applications [5], [6]. This is thanks to its fast torque response and robustness against machine parameter variations. Using hysteresis comparators and the switching vector table for both flux and torque control is the origin of its simple structure. However, a direct torque controlled motor suffers from great torque ripples due to the fast torque response. Many control algorithms have been proposed to reduce the torque ripple in DTC. A detailed survey of these methods can be found in [7]. Due to the direct relationship between the torque ripple and motor flux value [8], a DTC scheme combined with an efficiency optimizer increases the efficiency as well as generates smaller torque ripples than that found in conventional DTC.

This method has been applied to a DTC based induction motor drive and it has been shown that the torque ripple decreases [9]. It has also been shown that the torque ripple has a direct relation with the flux value through a complex relationship [8] and reducing the stator flux leads to the reduction of the torque ripple [10].

In this paper, the effect of flux reference value on the torque ripple in a DTC drive is reexamined in a

---

[*]Received by the editor January 8, 2006 and in final revised form July 7, 2008
[**]Corresponding author

more detailed way. In this study, the original equation for torque ripple presented in [8] is used and the variation of this relationship versus the flux value is investigated for a wide speed range.

In the next section a brief introduction about DTC in induction motors is presented. The motor torque ripple and the effect of the flux value on it are explained in section III. Simulation and experimental results are presented in sections IV and V, respectively.

2. DIRECT TORQUE CONTROL

The basic idea of the DTC concept, whose block diagram is shown in Fig. 1, is to choose the best vector of the voltage that makes the flux rotate and produce the desired torque. During this rotation, the amplitude of the flux rests in a pre-defined band. With a three-phase voltage source inverter, there are six non-zero voltage vectors and two zero voltage vectors that can be applied to the machine terminals as shown in Fig. 2.

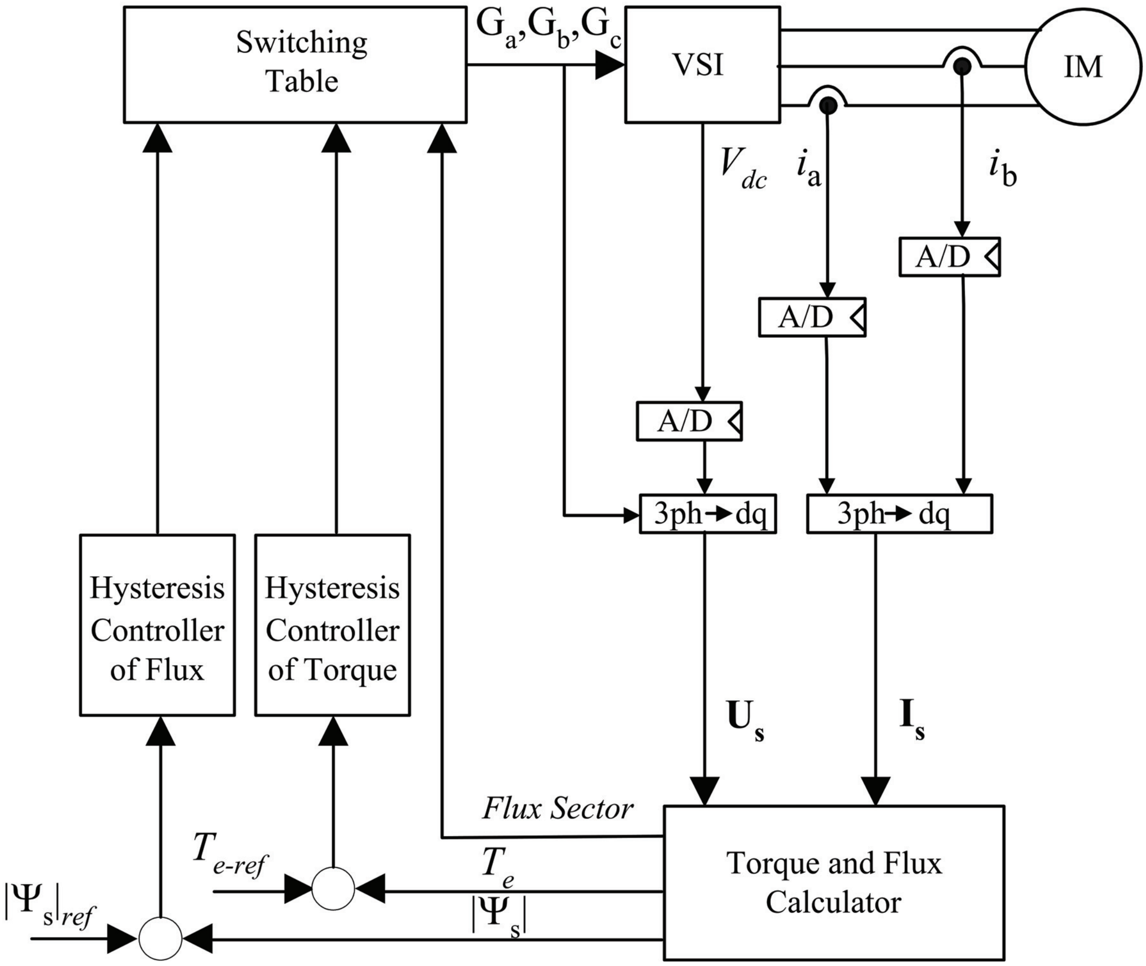

Fig. 1. Block diagram of the DTC method

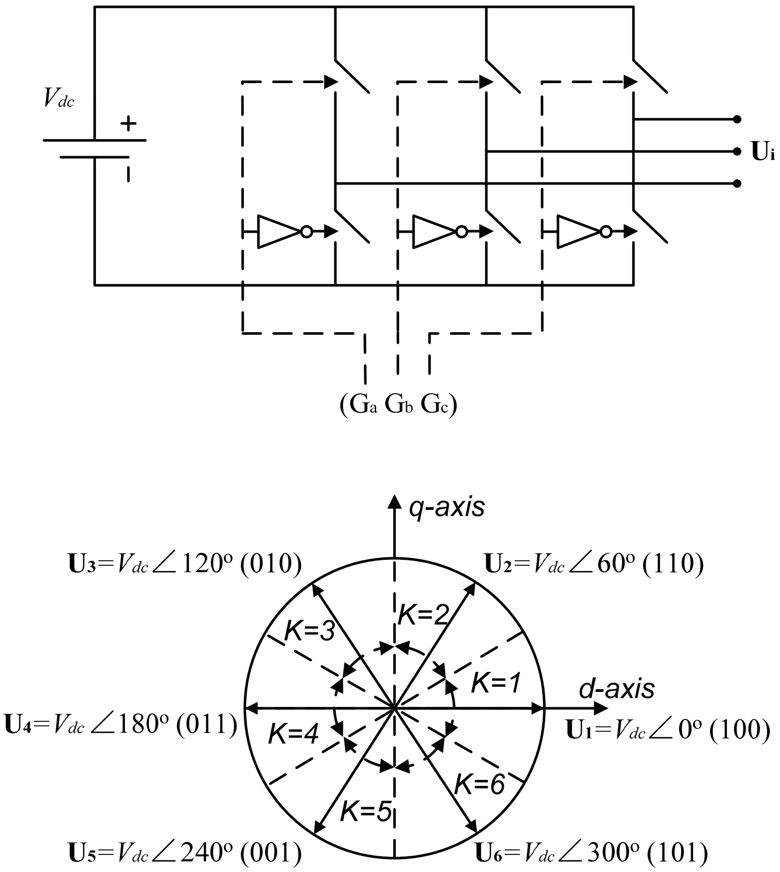

Fig. 2. Three phase two level inverter and its voltage vectors

The stator flux vector can be estimated using the measured current and voltage vectors:

$$\psi_s = \int (V_s - R_s I_s) dt \tag{1}$$

The torque can then be calculated using the components of the estimated flux and measured currents:

$$T_e = P(\psi_d I_q - \psi_q I_d) \tag{2}$$

Circular trajectory of the stator flux is divided into six symmetrical sections referred to as inverter voltage vectors. For each section, a proper vector set is proposed to maintain the amplitude of the flux and torque constant.

3. EFFECTS OF FLUX VALUE ON THE TORQUE RIPPLE

The most important characteristic of DTC is its fast torque response. When a non-zero voltage vector is applied to the motor, the stator flux vector rotates, the angle between the stator flux and the rotor flux changes, and the amplitude of the motor torque varies rapidly. Instantaneous torque error can jump out of the torque hysteresis band if the sampling period is not small enough. Therefore, the motor that is driven with DTC usually suffers from large torque ripple. This large torque ripple has an undesired effect on motor useful life and also on the load.

To analyze the important factors affecting torque dynamics, the torque ripple ΔT_e is divided into two parts as shown in the following equations [8].

$$\Delta T_e = \Delta T_1 + \Delta T_2 \tag{3}$$

Where

$$\Delta T_1 = -T_e(\frac{1}{\tau_s} + \frac{1}{\tau_r})\frac{T_s}{\sigma} \tag{4}$$

$$\Delta T_2 = P\frac{L_m}{\sigma L_s L_r}[(V_s - j\omega_m\psi_s) \bullet j\psi_r]T_s \tag{5}$$

The first component of torque variations (ΔT_1) is due to the stator and rotor resistances and decreases the absolute value of the torque. As can be seen in (4), this component is proportional to the torque and is independent of the voltage vector and motor speed. The second component of torque variations (ΔT_2) represents the effect of the applied voltage vector on the torque variation and depends on the motor speed. While the value of the motor flux has no effect on the first component of torque ripple, it mainly influences the second component. The effects of the motor flux on torque ripple at different speeds can be explained as shown below:

a) Low speed

At low speed ($\omega \approx 0$), the second torque ripple component (5) can be summarized as:

$$\Delta T_2 \approx P\frac{L_m}{\sigma L_s L_r}[V_s \bullet j\psi_r]T_s \tag{6}$$

On the other hand, the dynamic behavior of an induction machine with electric circuit diagram shown in Fig. 3 can be described by equations 7-10.

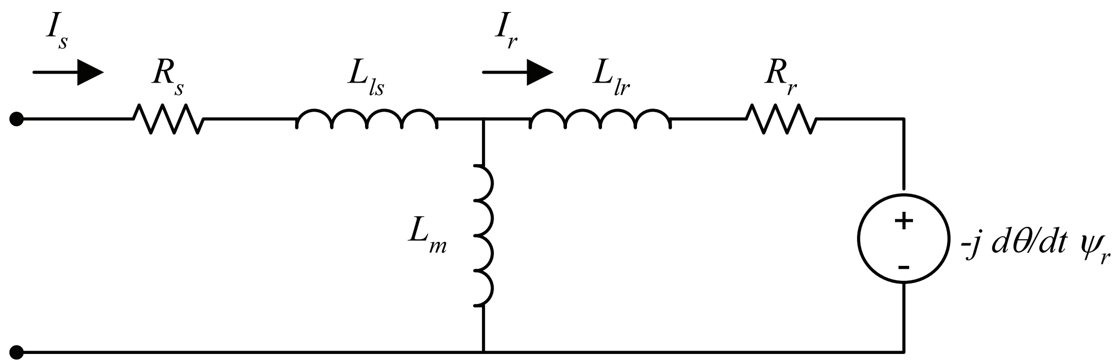

Fig. 3. The space vector circuit diagram of induction motor

$$V_s = R_s I_s + \frac{d\psi_s}{dt} \tag{7}$$

$$0 = R_r I_r + \frac{d\psi_r}{dt} - j\omega\psi_r \tag{8}$$

$$\psi_s = L_s I_s + L_m I_r \tag{9}$$

$$\psi_r = L_r I_r + L_m I_s \tag{10}$$

The waveform of the rotor flux, ψ_r, is very similar to its steady state waveform in DTC [9]. Therefore, (8) can be rewritten as

$$0 = R_r I_r + j\omega_s\psi_r - j\omega\psi_r \tag{11}$$

Using (9), (10) and (11), the rotor flux can be expressed as:

$$\psi_r = \frac{L_m R_r}{L_s R_r - j(L_m^2 - L_s L_r)(\omega - \omega_s)} \psi_s \tag{12}$$

According to equation (6), the maximum value of the second component of torque ripple is in the case that Ψs is perpendicular to Vs. Considering that ω is negligible, substituting the rotor flux from equation (12) results in:

$$\Delta T_{2\max} \approx P \frac{R_r L_m^2}{\sigma L_s L_r \sqrt{L_s^2 R_r^2 + \omega_s^2 (L_m^2 - L_s L_r)^2}} |V_s||\psi_s| T_s$$

$$= P \frac{R_r L_m^2}{\sigma L_s L_r \sqrt{L_s^2 R_r^2 + \omega_s^2 (L_m^2 - L_s L_r)^2}} V_{dc} |\psi_s| T_s \tag{13}$$

It can be seen that at low speeds, this component is a linear function of stator flux. Since the negative component of torque ripple is independent of the flux, the total torque ripple shows a linear variation with the stator flux. At light loads, the negative component which is proportional to the torque has a small value, and the second component becomes the dominant part. Therefore, the variation of torque ripple versus stator flux has greater slope at light loads than heavy loads.

b) High speed

For the stator flux values around its nominal value the second term of torque ripple can be summarized as follows:

$$\Delta T_2 = P \frac{L_m}{\sigma L_s L_r} [j\omega_m \psi_s \bullet j\psi_r] T_s \tag{14}$$

From (12), the maximum value of this term is proportional to the square of stator flux. Therefore, it shows a greater variation than that found at low speed.

For small values of stator flux the negative term can be expressed like (6). Therefore, it varies linearly with stator flux variations as explained in the previous section.

The negative component of torque is greater than the positive part at high speed. Therefore, the variation of total torque ripple versus stator flux has a smaller slope than that at low speed. However, when the motor load is very light, the negative term becomes very small so that the effect of the positive part is more obvious.

4. SIMULATION RESULTS

To show the independence of the theoretical results from the motor type, two different types of induction motors are used in these simulations. The parameters of the induction motors used in this study are shown in Tables 1 and 2. The value of the sampling interval in the simulations is 100 microseconds. The torque ripple factor in Eq. 12 is used for evaluating the quality of the torque ripple [8].

$$\delta = \sqrt{\frac{1}{T} \int_0^T \left(\frac{T_e}{T_{e-av}} - 1\right)^2 dt} \tag{15}$$

Table 1. Characteristics of induction motor A

Parameter	Value
Rated Power	370 W
Number of Poles	2
Stator Resistance	23 Ω
Stator Inductance	1.17 mH
Magnetizing Inductance	1.05 mH
Rotor Resistance	23 Ω
Rotor Inductance	1.17 mH
Nominal torque	1.2 N.m
Nominal flux	1.0 Wb

Table 2. Characteristics of induction motor B

Parameter	Value
Rated Power	5.5 kW
Number of Poles	4
Stator Resistance	0.18 Ω
Stator Inductance	56 mH
Magnetizing Inductance	53 mH
Rotor Resistance	0.5 Ω
Rotor Inductance	56 mH
Nominal torque	35 N.m
Nominal flux	0.65 Wb

Figure 4 shows the variation of torque ripple versus stator flux at low speed (100 RPM) for motor A. The lower value of the stator flux is limited to the stability margin of the motor. As expected, the torque ripple has a linear variation versus the stator flux and the slope of its variation is higher at light loads than that at heavy loads. Figure 5 shows the same behavior for motor B. Figures 6 and 7 show the variation of torque ripple versus stator flux at high speed (1500 RPM). As expected, the variation of torque ripple has a constant slope at heavy loads and becomes sharper at light loads. As mentioned before, at high speed the negative part of the torque ripple is dominant and independent of flux. Therefore, the variation of the torque ripple shows only a shift without any variation in the slope for heavy load. At light load, however, the negative part becomes small so that the effect of the stator flux is more obvious.

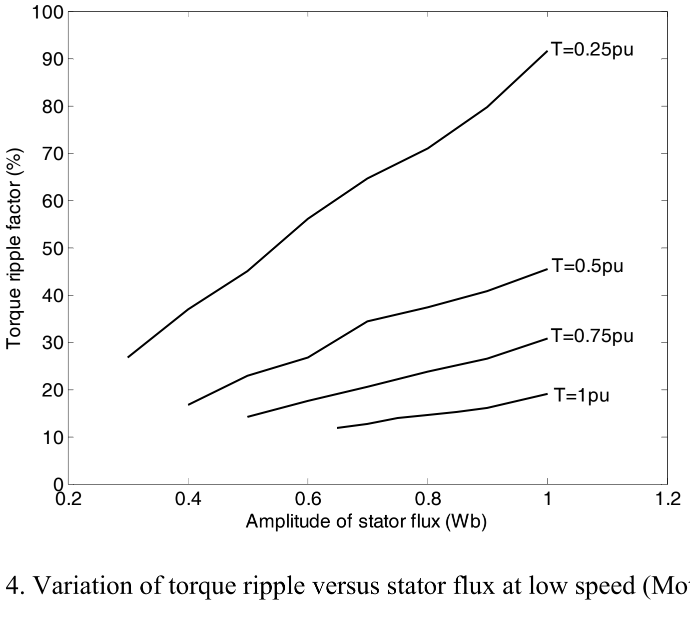

Fig. 4. Variation of torque ripple versus stator flux at low speed (Motor A)

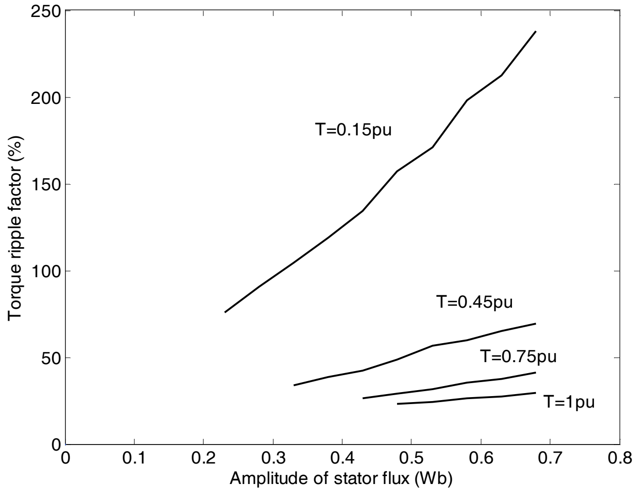

Fig. 5. Variation of torque ripple versus stator flux at low speed (Motor B)

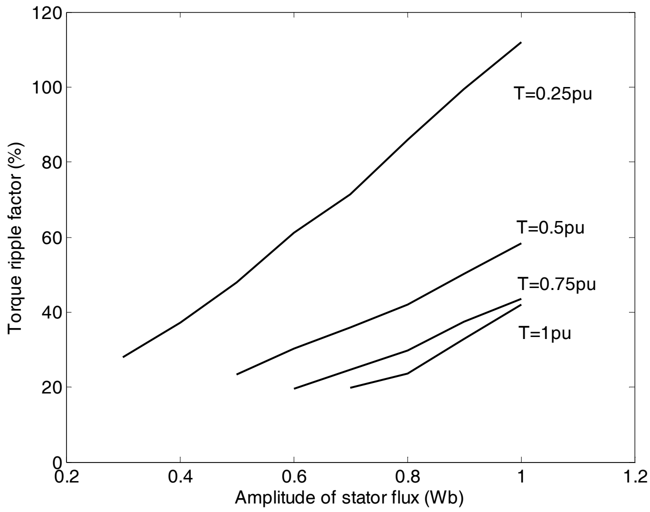

Fig. 6. Variation of torque ripple versus stator flux at high speed (Motor A)

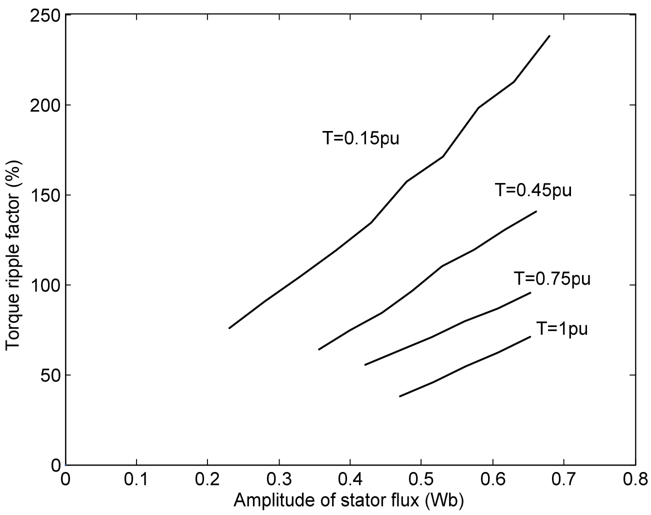

Fig. 7. Variation of torque ripple versus stator flux at high speed (Motor B)

5. EXPERIMENTAL RESULTS

To verify the computer simulation results, a proposed control method has been applied in a DTC experimental setup. The experimental setup, shown in Fig. 8, consists of a 0.37 KW induction motor, insulated gate bipolar transistor (IGBT) based inverter, and digital signal processor (DSP) (ADMC331)-based controller. The induction motor has the same parameters in simulation for motor A. The machine currents i_a and i_b and the dc bus voltage were interfaced into the controller through an analog to digital converter (A/D) built into the DSP board. The sampling frequency was set to 10 KHz and the DSP board was programmed by a PC.

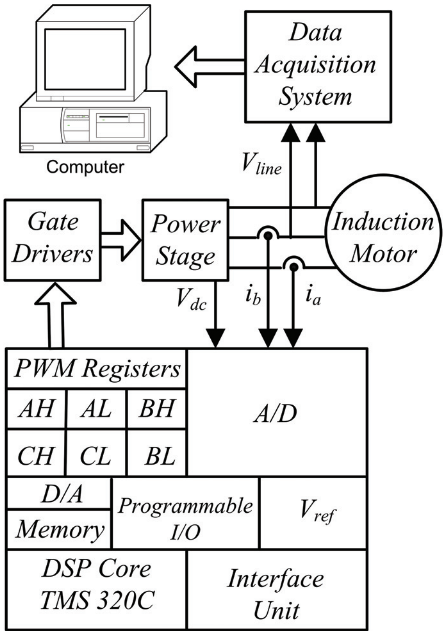

Fig. 8. Block diagram of experimental Setup

Figure 9 shows the variation of torque ripple versus stator flux at low speed. It can be seen that the slope of variation is small at heavy loads and it becomes sharper at light loads. This behavior is also seen in the torque ripple at high speed as shown in Fig. 10.

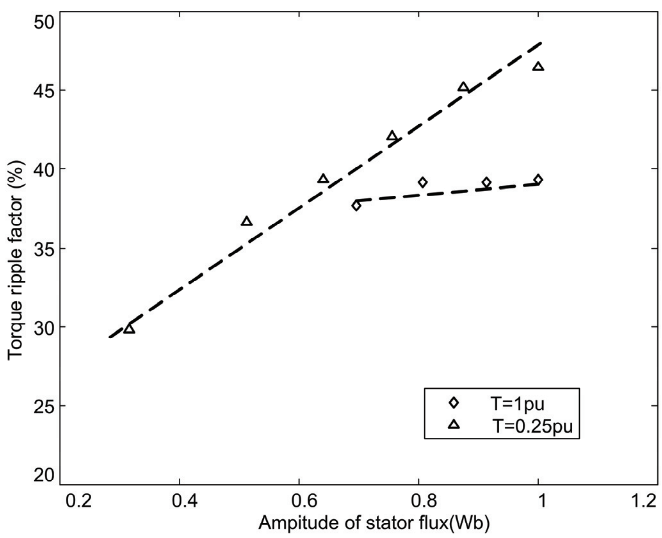

Fig. 9. Variation of torque ripple versus stator flux at low speed

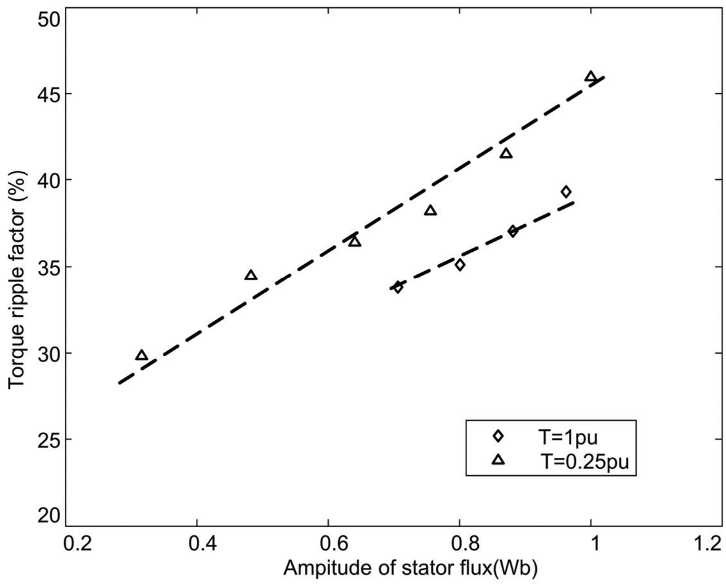

Fig. 10. Variation of torque ripple versus stator flux at high speed

6. CONCLUSIONS

The influence of the flux reference value on the torque ripple of a direct torque controlled induction motor has been investigated. Theoretical analysis and simulation and experimental results show that the variation of the torque ripple with the stator flux has great slope at light loads and smaller slope at heavy loads for both low and high speed. At low speed, the slope of the torque ripple is continuously varied with the motor load. But at high speed, this slope is almost constant for heavy load and varies when the motor works at very light load.

NOMENCLATURE

Ψ	Flux vector
I	Current vector
V	Voltage vector
T_e	Electromagnetic torque
ΔT_e	Torque ripple
T	Fundamental period of torque
τ	Time constant
T_s	Sampling time
p	Pole pair
L	Inductance
L_m	Mutual inductance
ω_m	Motor speed
V_{dc}	Inverter dc-link voltage
R	Winding resistance
$_{s}$, $_{r}$	Subscripts for stator and rotor quantities
$_{d}$, $_{q}$	Subscripts for direct and quadrate axis quantities
$_{av}$	Subscript for averaged quantities
σ	$1-L_m^2/L_sL_r$
δ	Ripple factor
•	Inner product

REFERENCES

1. Abrahamsen, F., Blabjeerg, F., Pedersen, J. & Theogersen, P. (2001). Efficiency-optimized control of medium-size induction motor drives. *IEEE Trans. Ind. App.*, *37*(6), 1761-1767.
2. Sousa, G., Bose, B. & Cleland, J. (1995). Fuzzy logic based on-line Efficiency optimization control of an indirect vector-controlled induction motor drive. *IEEE Trans. Ind. Elect.*, *42*(2), 192-198.
3. Takahashi, I. & Noguchi, T. (1986). A new quick-response and high-efficiency control strategy of an induction motor. *IEEE Trans. Ind. App, 22*(5), 820-827.
4. Depenbrock, M. (1988). Direct self-control (DSC) of inverter-fed induction machine. *IEEE Trans. Power. Elect, 3*(4), 420-429.
5. Schofield, J. R. G. (1995). Direct Torque Control-DTC. *ABB Ind. Sys*.
6. Trzynadlowski, A. M., Kazmierkowski, M. P., Grabowski, P. Z. & Bech, M. M. (1999). Three examples of DSP applications in advanced induction motor drives. *Proc. American Control Conf.* (2139-2140).
7. Kaboli, S. (2006). Optimization of Direct Torque Control for Reducing the Torque Ripple and Loss in Complete Set of Motor-Inverter. PhD Thesis, Sharif Univ. Tech.
8. Casadi, D., Serra, G. & Tani, A. (2000). Implementation of a direct torque control algorithm for induction motors based on discrete space vector modulation. *IEEE Trans. Power Elect, 15*(4), 769-777.
9. Kaboli, S., Zolghadri, M. R., Haghbin, S. & Emadi, A. (2003). Torque ripple minimization in DTC of induction motor based on optimized flux value determination. *IEEE Ind. Elec. Soc. Annual Meeting*, 431-435.
10. Kaboli, S., Zolghadri, M. R. & Homaifar, A. (2003). Effects of the flux value on the torque ripple of the direct torque controlled induction motor drives. *IEEE Power Elect. & Drive sys. Conf.* (439-444).